Back-Scattered Electron Visualization of Ferroelectric Domains in a $BiFeO_3$ Epitaxial Film

N. Alyabyeva[1, a)], A. Ouvrard[1], I. Lindfors-Vrejoiu[2], O. Ageev[3], and D. McGrouther[4]

[1] Institut des Sciences Moléculaires d'Orsay, CNRS, Université Paris-Saclay, F-91405 Orsay, France
[2] II. Physikalisches Institut, Universität zu Köln, 05937 Köln, Germany
[3] Research and Educational Centre "Nanotechnology", Southern Federal University, 347928, 2, Shevchenko Str., Taganrog, Russia
[4] School of Physics & Astronomy, University of Glasgow, Glasgow G12 8QQ, UK

[a)] Electronic mail: natalia.alyabyeva@u-psud.fr

ABSTRACT

Three-dimensional orientation of the ferroelectric (FE) domain structure of a $BiFeO_3$ epitaxial film was investigated by scanning electron microscopy (SEM) using back-scattered electrons and piezoresponse-force microscopy (PFM). By changing the crystallographic orientation of the sample and the electron collection angle relative to the detector, we establish a link between the orientation of polarization vectors (out-of-plane and in-plane) in $BiFeO_3$ film and the back-scattered electron image contrast in agreement with PFM investigations. The different FE polarization states in the domains correspond to altered crystalline environments for the impingent primary beam electrons. We postulate that the resultant back-scattered electron domain contrast arises as the result of either differential absorption (through a channelling effect) or through back-diffraction from the sample which leads to a projected diffraction pattern super-posed with the diffuse conventional back-scattered electron intensity. We demonstrate that SEM can be sensitive for both out-of-plane and in-plane polarization directions using BSE detection mode and can be used as a non-destructive and fast method to determine 3D FE polarization orientation of domains.

Keywords: Scanning electron microscopy, back-scattered electrons, ferroelectric domains, $BiFeO_3$ thin film, piezoresponse-force microscopy.

Introduction

One of the fundamental properties of ferroelectric (FE) materials is their spontaneous polarization. In $BiFeO_3$ (BFO), the spontaneous polarization at room temperature is about 100 $\mu C \cdot cm^{-2}$ along the $[111]_{pc}$[1,2] and can exhibit eight possible orientations, corresponding to upward and downward directions along the four pseudocubic (pc) perovskite structure diagonals.[1-4] Under an external electric field, the ferroelectric polarization can make orientation transitions of 180°, 109° and 71°.[2-4] Domain structures are composed of several unit cells having the same spontaneous polarization state, which can clearly be observed by different experimental methods like piezoresponse-force microscopy (PFM),[1,2,4-6] scanning electron microscopy (SEM),[6,7] transmission electron microscopy (TEM)[6,8] and low energy electron microscopy (LEEM).[9-11] PFM imaging is based on the converse piezoelectric effect, where an external electric field applied locally by a sharp metallic tip between the surface of the ferroelectric sample and the grounded bottom electrode induces mechanical expansions or contractions, detected as amplitude and phase changes of the cantilever oscillations. Despite its great advantage to probe FE domains, artefacts can appear in PFM imaging due to tip-surface electrostatic interactions.[12-14] SEM and TEM directly image the polarization charges, giving access to electrostatic topography.[6-8] The observed contrast is due to the change of electron emission properties (intensity, direction) from domains having a different polarization orientation.[15] SEM contrast obtained by back-scattered electrons (BSE) on crystalline samples can be induced by scattering geometry (electron diffraction and channelling) that can give access to ferroelectric[16,17] and ferromagnetic structure contrasts without being able to determine 3D polarization orientations.[18] High electron energies delivered by SEM and TEM can create defects, mostly oxygen vacancies (OV) that can modify the domain polarization[15] and even destroy ferroelectric thin films. Barrett's group uses very low energy electrons for domain manipulation and imaging with LEEM, without inducing OV as clearly shown for $BaTiO_3$(001) single crystals.[9] SEM and LEEM are mostly used to investigate ferroelectric domains on single crystals, while PFM and TEM have also been used on thin films.[4,5,8]

In this paper, we show that SEM can image both out-of-plane (OP) and in-plane (IP) domains in ferroelectric $BiFeO_3$ thin films, without inducing OV and destroying the film with a fast acquisition time by monitoring BSE. Crystallographic orientation of the sample (azimuth) and electron collection angle were tuned to determine the 3D orientation of the FE polarization vectors in the thin film with the support of PFM measurements.

Results

60 nm thick $BiFeO_3$ thin film was grown on $SrRuO_3$ buffer layer on $DyScO_3$(110) substrate by pulsed laser deposition (PLD) in a 0.14 mbar O_2 atmosphere with a substrate temperature of 650°C. Laser pulse energy of 90 mJ (energy density of 0.4 J/cm^2) was used, leading to a 0.5-1.5 nm/min growth rate.[19] Growth details of the BFO thin film and its crystallinity investigation by XRD are given elsewhere.[20]

The 3D orientation of the BFO film polarization vectors were determined by PFM and used as a reference to compare with SEM results. The study was carried out in high vacuum (<10^{-9} mbar), to reduce sample contamination in air which can increase electrostatic interactions in between the conductive cantilever (3 N/m mechanical stiffness) and the sample. 1 V_{ac} was applied to the cantilever to create a polarizing electric field. The modulation frequency was set off the 85 kHz resonance at 100 kHz to reduce the topography contribution while keeping a good enough PFM sensitivity.[21] OP and IP components of the piezoresponse were investigated along [100], [$0\bar{1}0$] and [$1\bar{1}0$] crystallographic orientations. In order to investigate the same region by SEM, a marker square was created (5 × 5 µm²) on the surface. The selected region was scanned in contact-mode under -4.5 V_{DC} and 1 V_{AC} tip bias voltage in analogy with acoustic microscopy.[22,23] This induced local switching of the polarization vector direction.

Following PFM characterization and polarization writing, SEM investigations were performed on unmetallized surfaces using a Nova NanoLab 600 platform (Co. FEI, Netherlands) under 10^{-6} mbar vacuum. Using the through lens detector (TLD), electrons originating from a narrow angular range about the specimen surface normal were detected.[24] Suction tube voltage was negative, allowing the repulsion of low energy secondary electrons from the TLD detector and therefore the detection only of back-scattered electrons. EB was set at 5 keV and 0.4 nA. In addition, the use of larger EB radius (62 nm) and fast acquisition time (17.1 µm (1 line) per µs) minimizes irradiation damages and image drifting while maintaining a good spatial resolution.[17,24] OP and IP polarized FE domains in the BFO film were investigated along the main crystallographic orientations ([100], [$0\bar{1}0$] and [$1\bar{1}0$]), by changing specimen azimuth angle, for two EB incident angles (θ = 0° and 15° relative to sample normal).

Figure 1 presents PFM measurements of piezoresponse of the unmodified BFO surface and the square area. Four types of domains were observed: (i) stripe domains (D_1 and D_2) in unmodified

area; (ii) domains with switched polarization vectors (D_S) and (iii) additional domains (D_A) rotated by 90° relative to the others. **Figure 1(a)** shows the induced normal sample displacements, giving a direct access to OP piezoresponse distribution of the FE domains along the [100] direction. Bright regions (D_1, D_2 and D_A) correspond to positively charged domains, *i.e* upward polarization vector (positive phase shift), while dark ones (D_S) correspond to negatively charged domains, *i.e* downward polarization vector (negative phase shift). PFM images of the OP response along other crystallographic orientations are identical (not presented here), since the normal piezoresponse is independent on the crystallographic direction. In **Figure 1(b-d)** are shown the induced lateral sample displacements, giving a direct access to the IP piezoresponse distribution of the FE domains along [100], [$0\bar{1}0$], [$1\bar{1}0$] directions, respectively. Bright regions (D_1 in **Figure 1(b-d)**; D_2 and D_S in **Figure 1(b)**) correspond to rightward IP piezoresponse direction (positive phase shift). Dark regions (D_A in **Figure 1(b-d)**; D_2 and D_S in **Figure 1(c)**) correspond to the leftward IP piezoresponse direction (negative phase shift). Domains D_2 and D_S in **Figure 1(d)** have a weaker contrast in comparison with D_1 and D_A, because polarization vectors are collinear to the scan line direction.

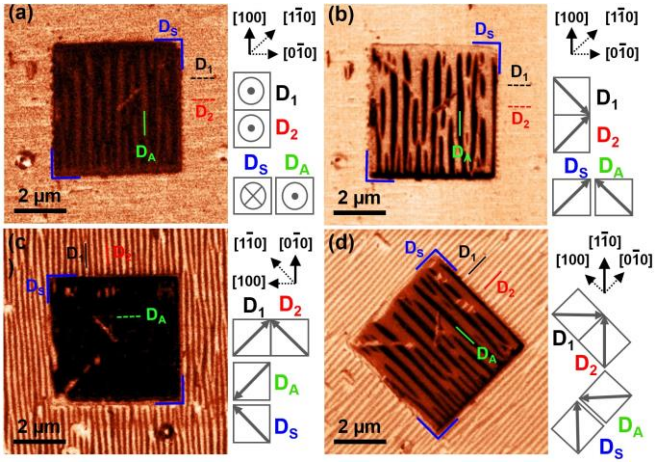

FIG. 1. PFM images of polarized FE domains in the unmodified/modified BFO thin film: (a) OP components for a scan perpendicular to [100] orientation; (b-d) IP components for scans perpendicular to [100], [$0\bar{1}0$], [$1\bar{1}0$] orientations, respectively. Beside each PFM image is given a schematic representation of OP (a) and IP (b-d) components. All domains are highlighted by lines: black (D_1), red (D_2), blue (D_S), and green (D_A). Dotted lines indicate not visible domains.

The 2D representation of the OP and IP components can be deduced from this analysis and they are given in **Figure 1** beside each PFM image. OP and IP polarization vector directions were deduced from PFM measurements allowing determination of the 3D orientation of the different domains in the unmodified and modified BFO thin film [**Fig. SM-1**]. A polarization orientation

difference of 71° was found for pair domains (D_1, D_2), (D_2, D_A) and (D_2, D_S) and 109° for (D_1, D_A), (D_1, D_S) and (D_A, D_S). The relative orientation of D_1 and D_2 is in a good agreement with literature.[2-4,19,20] Non-180° switching towards D_S and D_A with opposite polarity is unexpected and can be interpreted as symmetry breaking probably involving the "contact-oscillation" mode used during polarization switching. Previously symmetry breaking in BFO thin film was reported by the group of Kalinin,[25] where the rotationally invariant tip field in an SPM experiment promoted breaking of the IP symmetry.

SEM images were obtained on the BFO thin film for the same region investigated by PFM, for different sample azimuth angles ([100], $[0\bar{1}0]$ and $[1\bar{1}0]$ directions) and with the EB incidence angles shown in **Figure 2**. Domains D_1, D_2, D_S and D_A are highlighted as in PFM images [**Fig. 1**].

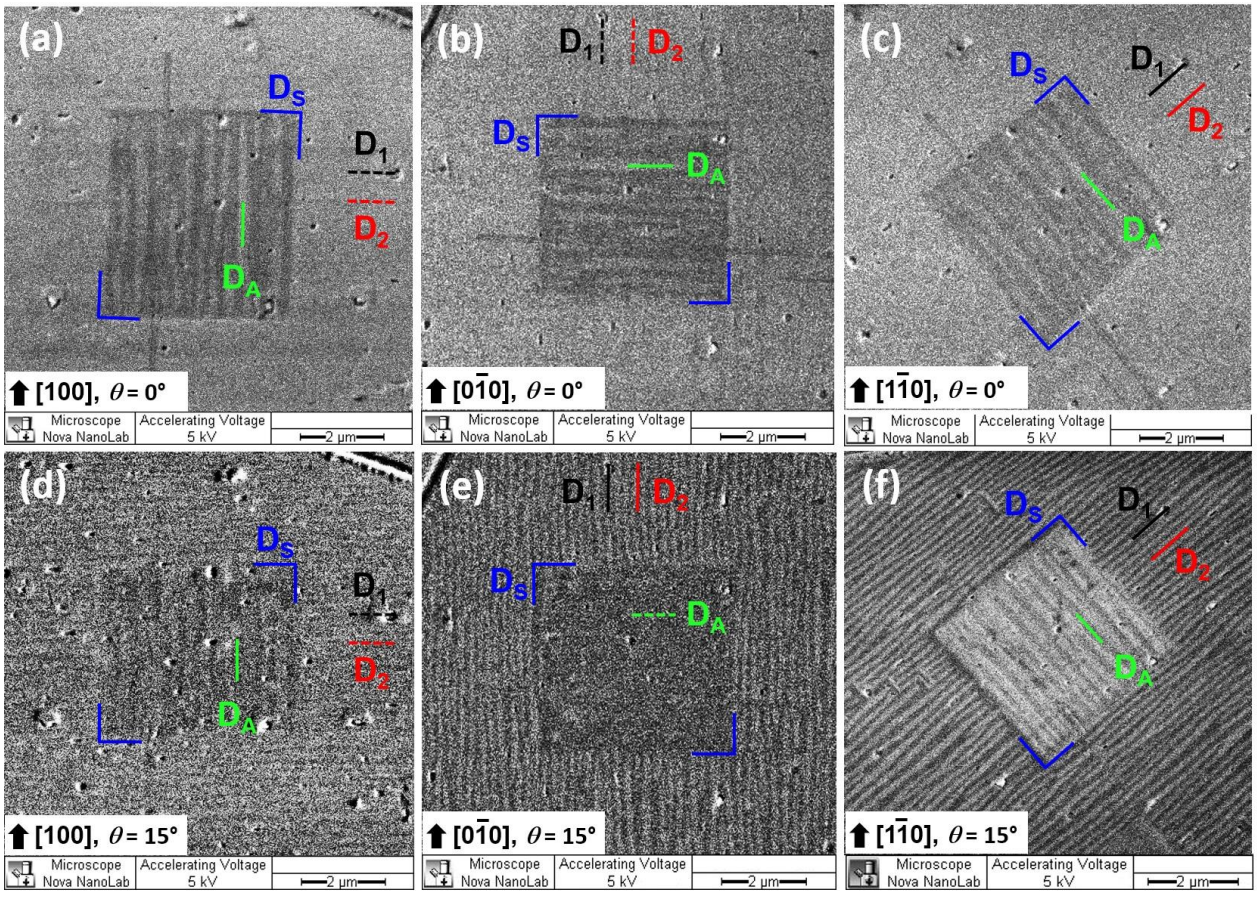

FIG. 2. SEM images of polarized FE domains determined by BSE monitoring in BFO thin film for three sample azimuth angles ([100]: (a) and (d), $[0\bar{1}0]$: (b) and (e), $[1\bar{1}0]$: (c) and (f)) and different incidence angle (θ) relative to surface normal: (a-c) – 0°; (d-f) – 15°. All domains are highlighted by lines as in **Figure 1**.

Domain contrast was observed at all azimuth angles and globally decreased with incidence angles (θ). At normal incidence, domain contrast was independent of the specimen azimuth, D_S

intensity was always lower (darker) than the others, while D_1, D_2 and D_A did not show any intensity variation [**Fig. 2(a-c)**]. Tilting the sample to $\theta = 15°$ from the normal, resulted in variation of the relative domain contrast, now strongly dependent upon the azimuth angle [**Fig. 2(d-f)**]. A significant intensity contrast has appeared for the unmodified (D_1, D_2) and modified (D_S, D_A) domains. Profiles across pair domains (D_1, D_2) and (D_S, D_A) [**Fig. 3**] show their contrast dependency to the EB incident angle, as well as their good correlation with PFM results. Domain widths of 100±20 nm for (D_1, D_2) [**Fig. 3(b)**] and 200±50 nm for (D_S, D_A) [**Fig. 3(c, d)**], exactly twice D_1 or D_2 widths were observed. It shows that D_1 and D_2 were switched locally by pair into D_A. Domain boundary sizes are approximately 50±20 nm for all domains imaged by both SEM or PFM, *i.e.* much more spatially extended than the spatial resolution of both instruments.[26]

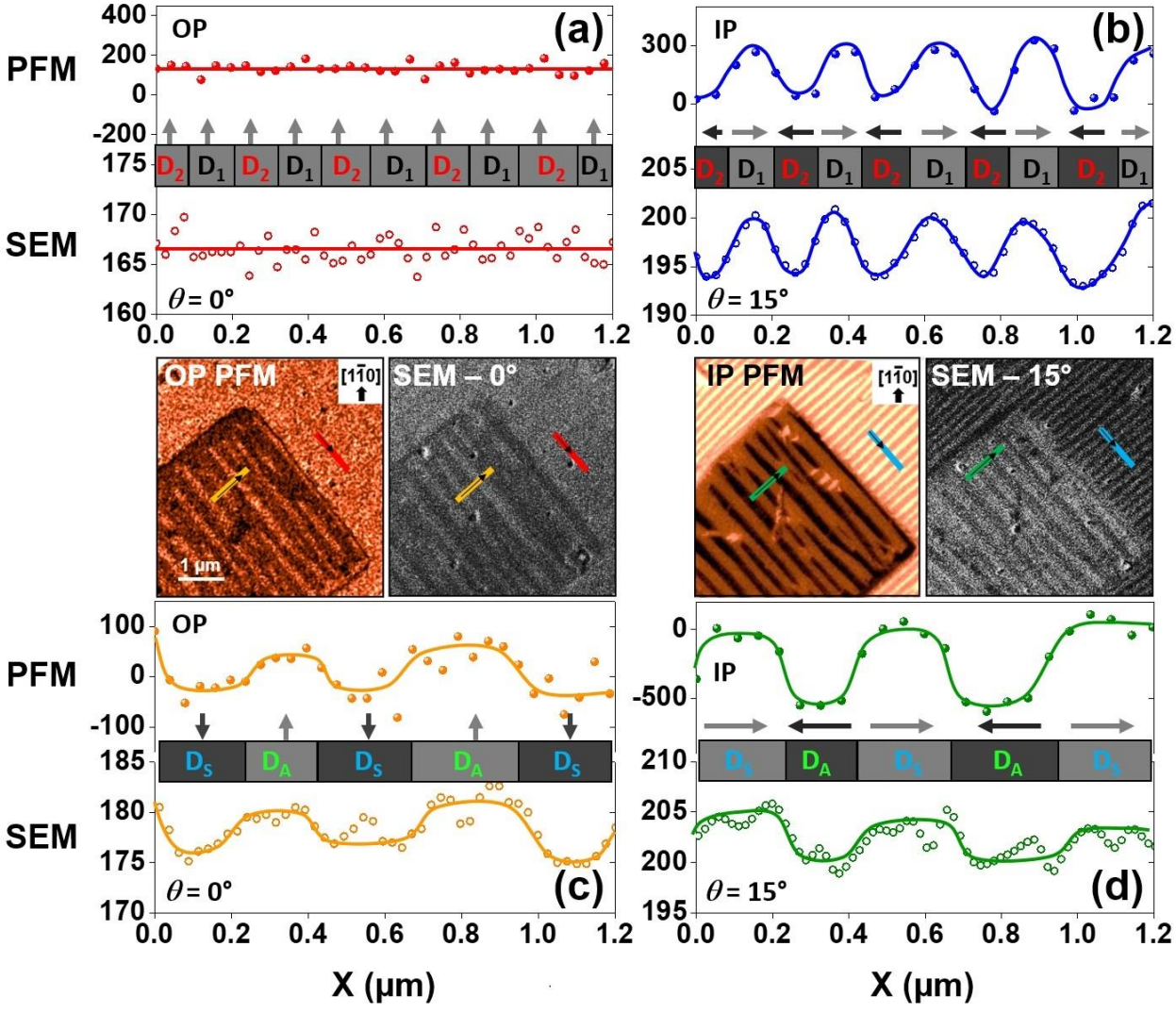

FIG. 3. PFM and SEM intensity profiles along colour lines represented in PFM and SEM images for (a, b) D_1, D_2 and (c, d) D_S, D_A. Polarization vector representation is given for all domains.

Current intensity of each domain for the three azimuth and incidence angles are gathered in **Figure SM-2** and compared to out-of-plane and in-plane contrasts of PFM results. At normal incidence, SEM results were very similar to OP PFM results [**Fig. 3(a, c)**]. According to PFM measurements, only D_S domains were downward polarized [**Fig. SM-1**], corresponding in SEM to a lower BSE current at all azimuths. It suggests that SEM at normal incidence is only sensitive to the OP component of the piezoresponse. At θ = 15°, azimuth angle strongly influenced the BSE contrast [**Fig. 2(d-f)**]. For [100] azimuth, scattered current by D_A was smaller than D_1, D_2 and D_S. For this azimuth, IP PFM showed negative shift only for D_A indicating a leftward pointing polarization vector. For $[0\bar{1}0]$ azimuth, D_2, D_S and D_A showed lower intensity in comparison with D_1 by SEM, while IP PFM showed a rightward polarization for D_1 and a leftward polarization for others. For $[1\bar{1}0]$ azimuth, all domains had different scattered current (D_1>D_2 and D_S>D_A). The SEM/PFM correlation is clear for D_1 and D_A [**Fig. 3(b, d)**]. Concerning D_2 and D_S, PFM is not sensitive to in-plane component (polarization is collinear to the cantilever) and cannot be compared to SEM. Similarity of SEM contrasts with IP PFM measurements allows suggesting that at θ = 15°, SEM is sensitive to IP component.

Discussion

Based on the correlation between SEM and PFM measurements, we conclude that at normal incidence BSE is sensitive to the OP piezoresponse. For EB angles away from normal incidence, in-plane components contribute to the contrast in SEM and being azimuth dependent they are in very good agreement with PFM results. Both OP and IP sensitivity of SEM were hitherto unexpected for the BSE imaging mode. The observed contrast in BSE mode could arise from two possible sources:

(i) BSE contrast is known to depend classically on atomic weight, specimen tilt (EB incidence), EB energy and relatively weakly upon crystallographic directions (electron channelling).[17,24] In our case, atomic weight and macroscopic crystallographic directions are homogeneous across the different domains. Microscopically, electron diffraction and channelling within the crystalline films can be sensitive to minute strain induced distortions arising from ferroelectric domains as reported recently using SEM and BSE monitoring and lead to an anisotropic BSE angular distribution.[16-18]

(ii) Originating from an alternative mechanism, the observed contrast could be linked to the backwards oriented-diffraction from the sample which leads to a projected diffraction pattern super-imposed with the diffuse conventional back-scattered electron intensity. Scanning across ferroelectric domains will result pattern geometry and intensity variations which may be detected by our TLD detector sampling a small area of the pattern. Support for this idea comes from the early EB diffraction work of Alam *et al.*,[27] which demonstrates that the commonly used electron backscatter diffraction orientation (EB ~70° incidence to surface normal) produces strong scattering but those patterns also exist at high angles back along the incident beam direction. For all EB diffraction from bulk samples there is combined diffuse and elastic scattering, which gives rise to the Kikuchi bands in diffraction patterns.[28]

Thus, the obtained results show that SEM tool, for specific incidence and azimuth angles is sensitive to both out-of-plane and in-plane components of the FE piezoresponse. Development of a clear explanation for the contrast origin would make SEM a powerful technique for OP and IP piezoresponse investigations. This technique could be applied for other piezoelectric materials including thin films, but it may require modifications of EB setting parameters (energy, scanned length and speed) and incidence angle. Visualizing ferroelectric domains by SEM with strong contrast will facilitate observation of dynamic domain behaviours with timescales (~milliseconds) far faster than accessible with the current de-facto standard PFM imaging technique.

Conclusion

Ferroelectric $BiFeO_3$ epitaxial films have been investigated by SEM and PFM. A very good agreement is found between both methods. SEM domain contrast is specimen tilt- and azimuth angle- dependent allowing to determine both out-of-plane and in-plane polarization directions. We suggest that the FE polarization of the different domains change the BSE detection efficiency due to an anisotropic emitted electron angular distribution. We demonstrate, that SEM using BSE detection mode can be used as a sensitive, non-destructive and fast method to determine 3D polarization orientations in ferroelectric thin films.

Supplementary Material

See supplementary material for the determination of the 3D orientation of domain polarization vectors, the quantitative analysis of SEM and PFM results and the discussion of the reproducibility of SEM results and their correlation with PFM.

Acknowledgments

This work was conducted in collaboration with Materials and Condensed Matter Physics Group, University of Glasgow, UK and Research and Educational Centre "Nanotechnology", Southern Federal University, Russia. We gratefully acknowledge Dr. Antoine Ruyter and Dr. Carol Trager-Cowan for insightful participation in scientific discussions.

References

[1]P. Rovillain, R. de Sousa, Y. Gallais, A. Sacuto, M. A. Méasson, D. Colson, A. Forget, M. Bibes, A. Barthélémy, and M. Cazayous, Nat. Mater. **9**, 975–979 (2010).

[2]S.-H. Baek, C. M. Folkman, J.-W. Park, S. Lee, C.-W. Bark, T. Tybell, and C.-B. Eom, Adv. Mater. **23**, 1621–1625 (2011).

[3]S. H. Baek, H.W. Jang, C. M. Folkman, Y. L. Li, B. Winchester, J. X. Zhang, Q. He, Y. H. Chu, C. T. Nelson, M. S. Rzchowski, X. Q. Pan, R. Ramesh, L. Q. Chen, and C. B. Eom, Nat. Mater. **9**, 309–314 (2010).

[4]T. Zhao, A. Scholl, F. Zavaliche, K. Lee, M. Barry, A. Doran, M. P. Cruz, Y. H. Chu, C. Ederer, N. A. Spaldin, R. R. Das, D. M. Kim, S. H. Baek, C. B. Eom, and R. Ramesh, Nat. Mater. **5**, 823 - 829 (2006).

[5]Y. H. Chu, T. Zhao, M. P. Cruz, Q. Zhan, P. L. Yang, L. W. Martin, M. Huijben, C. H. Yang, F. Zavaliche, H. Zheng, and R. Ramesh, Appl. Phys. Lett. **90**, 252906 (2007).

[6]M. Bah, N. Alyabyeva, R. Retoux, F. Giovannelli, M. Zaghrioui, A. Ruyter, F. Delormea, and I. Monot-Laffez, RSC Adv., **6**, 49060-49067 (2016).

[7]G. Rosenman, A. Skliar, I. Lareah, N. Angert, M. Tseitlin, and M. Roth, Phys. Rev. B. **54**, 9 (1996).

[8]Y. B. Chen, M. B. Katz, X. Q. Pana, R. R. Das, D. M. Kim, S. H. Baek, and C. B. Eom, Appl. Phys. Lett. **90**, 072907 (2007).

[9]J. E. Rault, T. O. Mentes, A. Locatelli, and N. Barrett, Scientific Reports **4**, 6792 (2014).

[10]S. Cherifi, R. Hertel, S. Fusil, H. Béa, K. Bouzehouane, J. Allibe, M. Bibes, and A. Barthélémy, Phys. stat. sol. (RRL) **4**, 22–24 (2010).

[11]J. L. Wang, B. Vilquin, and N. Barrett, Appl. Phys. Lett. **101**, 092902 (2012).

[12]S. Jesse, A. P Baddorf, and S. V. Kalinin, Nanotechnology **17,** 1615–1628 (2006).

[13]S. V. Kalinin, and D. A. Bonnell, Phys. Rev. B **65**, 125408 (2002).

[14]L. F. Henrichs, J. Bennett, and A. J. Bell, Rev. Sci. Instrum. **86**, 083707 (2015).

[15]D. Li, and D. A. Bonnell, Ann. Rev. Mater. Res. **38**, 351–368 (2008).

[16]G. R. Booker, A. M. B. Shaw, M.J. Whelan, and P.B. Hirsch, Philosop. Mag. **16**, 144, 1185-1191 (1967).

[17]D. Gruner, and Z. Shen, J. Am. Ceram. Soc. **93**, 48 (2010).

[18]J. Unguris, S. R. Bowden, D. T. Pierce, M. Trassin, R. Ramesh, S.-W. Cheong, S. Fackler, and I. Takeuchi, Appl. Phys. Lett. Mater. **2**, 076109 (2014).

[19]F. Johann, A. Morelli, and I. Vrejoiu. Phys. Status Solidi B **249**, 11, 2278–2286 (2012).

[20]F. Johann, A. Morelli, D. Biggemann, M. Arredondo, and Ionela Vrejoiu. Phys. Rev. B **84**, 094105 (2011).

[21]R. Proksch, and S. Kalinin. Asylum Res. PFM, app note **10** (*www.asylumresearch.com*).

[22]U. Rabe, K. Janser, and W. Arnold. Rev. Sci. Instrum. **67**, 9 (1996).

[23]S. Amelio, A.V. Goldade, U. Rabe, V. Scherer, B. Bhushan, and W. Arnold. Thin Sol. Fil. **392** ,75-84 (2001).

[24]J. I. Goldstein, D. E. Newbury, P. Echlin, D. C. Joy, C. E. Lyman, E. Lifshin, L. Sawyer, and J.R. Michael, Kluwer Academic/Phenum Publishers, New York (2003).

[25]N. Balke, S. Choudhury, S. Jesse, M. Huijben, Y. H. Chu, A. P. Baddorf, L. Q. Chen, R. Ramesh, and S. V. Kalinin. Nature Nanotechnology **4**, 868 (2009).

[26]S. V. Kalinin, S. Jesse, B. J. Rodriguez, J. Shin, A. P. Baddorf, H. N. Lee, A. Borisevich, and S. J. Pennycook. Nanotechnology **17,** 3400–3411 (2006).

[27]M. N. Alam, M. Blackman, and D. W. Pashley. Royal Society of London. Series A, Math.l and Phys. Sci. (1954).

[28]D. Bouscaud, A. Morawiec, R. Pesci, S. Berveiller, and E. Patoor. J. of App. Cryst. **47**, 5, 1479–1806 (2014).